

## Original articles

Research article

<https://doi.org/10.17308/kcmf.2024.26/12451>

## Labile states are the basis of functional materials

P. P. Fedorov✉

*Prokhorov General Physics Institute of the Russian Academy of Sciences,  
38 Vavilova st., Moscow 119991, Russian Federation*

### Abstract

The available data refute the widespread postulate of thermodynamics, according to which labile states are physically unrealizable, unobservable and, thus, devoid of practical interest, since the transition to a stable state does not require overcoming a potential barrier, and a random fluctuation leads to an accelerated shift of the system from the initial state. The cases when a system remains in a labile state for an indefinite period of time are well known. The corresponding states are not only observable, but can be used to create functional materials.

The article analyses low-temperature phase equilibria and spinodal behavior in a number of binary systems containing solid solutions with a fluorite structure, such as  $\text{CaF}_2\text{-SrF}_2$ ,  $\text{CaF}_2\text{-BaF}_2$ ,  $\text{BaF}_2\text{-RF}_3$  ( $R = \text{La, Nd}$ ),  $\text{SrF}_2\text{-LaF}_3$ ,  $\text{ZrO}_2\text{-Y}_2\text{O}_3$ . The investigation of low temperature phase formation in the  $\text{BaF}_2\text{-LaF}_3$  system allowed to reveal the decomposition of the solid solution  $\text{Ba}_{1-x}\text{La}_x\text{F}_{2+x}$  with a binodal curve. In the  $\text{SrF}_2\text{-LaF}_3$  system the equilibrium solubility curve of lanthanum fluoride in strontium fluoride is expressed at the inflection point on the solvus curve with a practically horizontal tangent, which corresponds to the bifurcation point – the practical coincidence of the critical point of the nonequilibrium binodal/spinodal with the solvus curve. The  $\text{Ba}_{1-x}\text{Ca}_x\text{F}_2$  continuous solid solution obtained by the mechanochemical method and possessing high fluorine-ion conductivity, remains in a labile state for an indefinitely long period of time. Upon heating, it disintegrates with an exothermic effect at 420–450 °C. In all other fluoride systems, single crystals grown from the melt retain the functional characteristics of photonics materials for years and have no signs of degradation.

Obviously, the technological stability of crystalline samples of the listed solid solutions is determined by the extremely low values of the cation diffusion coefficients. The systems are “falling”, but too slowly to detect it. The fine architecture of materials in a labile state is of considerable interest.

**Keywords:** Phase diagrams, Stability, Spinodal, Architecture of spinodal decomposition

**Funding:** The study was funded by a grant Russian Science Foundation No. 22-13-00167, <https://rscf.ru/project/22-13-00167>

**Acknowledgements:** The author is grateful to A. V. Naumov, A. I. Popov, V. V. Gusarov for discussing the problem, A. A. Alexandrov and A. A. Luginina for conducting the experiments.

**For citation:** Fedorov P. P. Labile states are the basis of functional materials. *Condensed Matter and Interphases*. 2024;26(4): 772–781. <https://doi.org/10.17308/kcmf.2024.26/12451>

**Для цитирования:** Федоров П. П. Лабильные состояния – основа функциональных материалов. *Конденсированные среды и межфазные границы*. 2024;26(4): 772–781. <https://doi.org/10.17308/kcmf.2024.26/12451>

✉ Pavel P. Fedorov, e-mail: [ppfedorov@yandex.ru](mailto:ppfedorov@yandex.ru)

© Fedorov P. P., 2024



The content is available under Creative Commons Attribution 4.0 License.

## 1. Introduction

It is known that a system is in equilibrium if it has a minimum of free energy and a maximum of entropy. A stable thermodynamic equilibrium should comply with following inequalities according to thermodynamics [1-3]:

$$C_p > C_v > 0 \quad (1)$$

(thermal stability),

$$\chi_T > \chi_S > 0 \quad (2)$$

(mechanical stability),

$$(\partial^2 G / \partial x^2)_{P,T} = (\partial \mu / \partial x)_{P,T} > 0 \quad (3)$$

(resistance to diffusion).

In these inequalities  $P$  – pressure,  $T$  – temperature,  $V$  – volume,  $C$  – heat capacity,  $S$  – entropy,  $G$  – isobaric-isothermal potential,  $\chi = (\partial P / \partial V)$  – compressibility,  $\mu$  – chemical potential,  $x$  – concentration.

Thermodynamics distinguishes three types of equilibria: stable, metastable, and labile. Metastable equilibria are locally stable (satisfy inequalities 1–3), but may be unstable with respect to the appearance of other phases. For the transition into the stable state, the system must overcome a potential barrier. Labile states are locally unstable (one of the inequalities 1–3 is impaired), and the transition to a stable (or metastable) state does not require overcoming a potential barrier.

As for labile equilibria, the thermodynamic literature accepts as a postulate that labile states are not physically realizable, at least not observable, and thus are devoid of practical interest, since the transition to a stable state does not require overcoming a potential barrier, and a random fluctuation leads to an accelerated shift of the system from the initial state.

“If within a certain interval of parameter values any of the inequalities (*stability criteria*) is not satisfied, then this interval cannot be associated with any really existing states.... Such states... are completely unstable (labile) and, therefore, physically impossible (in any case, unobservable).” [4, p. 74].

“Unstable states are practically unrealizable, since the slightest fluctuations shift the system out of the equilibrium state. Therefore, the use of stability conditions allows to identify real systems

and exclude systems that are devoid of practical interest.” [5, p. 44].

“Unstable equilibrium is not physically realizable. This statement is often questioned based on phenomenological reasoning, but it can be proven by statistical thermodynamics methods.” [6, p. 83].

“We obtain a curve on which thermodynamic inequalities are impaired (for a homogeneous body); it limits the region in which the body under no circumstances can exist as homogeneous.” [7, p. 285].

It should be noted that J. W. Gibbs, who actually formulated these stability criteria, expressed them much more cautiously: “A phase which is unstable with respect to continuous changes is evidently incapable of permanent existence on a large scale except in consequence of passive resistances to change” [1, p. 109].

The purpose of this study is the demonstration of the fallaciousness of these statements [4–7]. Systems in labile states are not only observable but also very useful from a practical point of view in materials science.

## 2. Problem statement

The set of points at which the stability conditions are impaired is called spinodal. The spinodal dimension (point, line or surface) can be different depending on the dimension of the corresponding phase diagram.

In general, determination of the position of spinodals requires the consideration of the thermodynamic model of the system. We will limit ourselves to considering the chemical spinodal, namely, considering the decomposition of solid solutions, i.e., the impairment of the stability of the system in relation to diffusion. According to the third law of thermodynamics, as the temperature decreases, phases of variable composition must undergo decomposition or ordering. We will limit ourselves to binary systems, which does not affect the generality of the conclusions.

At the same time, the position of the binodal, which is determined quite simply, allows to estimate the position of the spinodal with a high degree of reliability. In the immiscibility of solid solutions, the critical point, the binodal dome point  $K$  also belong to the spinodal, see Fig. 1. At

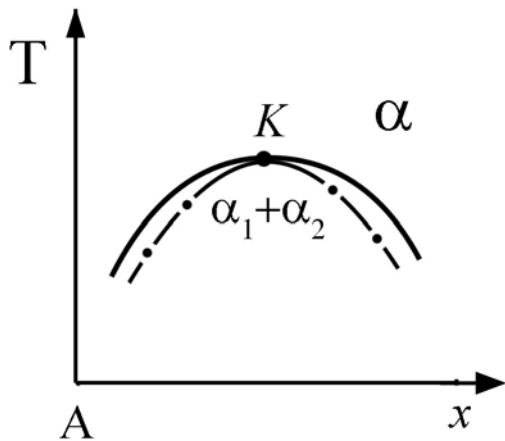


**Fig. 1.** Binodal and spinodal (dash-dotted line) during immiscibility of a solid solution in a binary system in the vicinity of the critical immiscibility point *K*

this point, both the binodal and the spinodal have a common horizontal tangent, i.e.  $(\partial T/\partial x)_p = 0$ .

There is a simple thermodynamic model, namely the regular solution model, applicable only to systems with isostructural components, but allows to qualitatively navigate in more complex cases. In the regular solution model for a binary system, the spinodal equation is written as follows [3]:

$$T = 4T_c x(1 - x), \tag{4}$$

where  $T_c$  – the absolute temperature of the critical point, which is realized at a composition containing 50 mol. % of components (Fig. 2a). At  $T \rightarrow 0$  K, the spinodal curve goes to the origin of

coordinates, but, unlike the binodal, does not have a vertical tangent at this point (Fig. 2). It should be noted that in the monograph by Prigogine and Defey the position of the spinodal is depicted with an error [3, Fig. 16.16]. Taking into account elastic stresses during the decomposition of solid solutions leads to a shift in the position of binodals and spinodals in the composition-temperature coordinates [8–10].

The immiscibility, i.e. the appearance of both the binodal and the spinodal associated with it, in the metastable region of existence of a solid solution or glass is of great interest [11, 12].

Experimental methods for determination of the position of spinodals are limited and generally effective only for relatively fast kinetics of phase transformations [13, 14]. The change in the microstructure of alloys can be used as a method for determining the spinodal [12]. The study [15] also deserves attention (the experimentally obtained region of solid solution immiscibility exactly corresponds to the spinodal equation).

### 3. Examples

The  $\text{CaF}_2\text{-SrF}_2$  system. The phase diagram is presented in Fig. 3 [16]. There is a continuous series of solid solution between isostructural components. The position of the critical point of decomposition of the solid solution is outlined based on the data of the study of the  $\text{CaF}_2\text{-SrF}_2\text{-MnF}_2$  ternary system [17]. At room temperature,

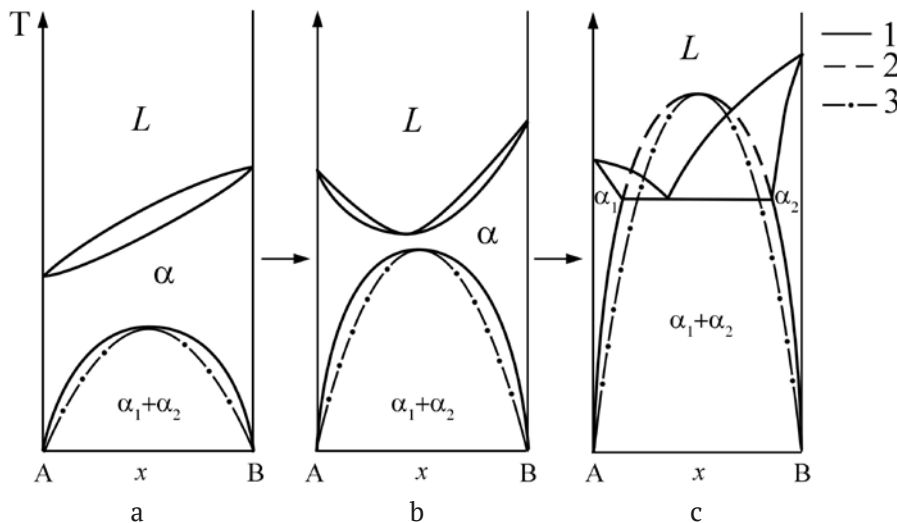


**Fig. 2.** Position of binodals and spinodals (dash-dotted line) in binary systems in the regular solution model. *L* – melt,  $\alpha$  – stratifying solid solution

only solid solutions containing up to 10 mol. % of the second component, while intermediate compositions containing 10-90%  $\text{CaF}_2$ , are in a labile state.

Nevertheless, the corresponding compositions can be grown in the form of single crystals and are recommended as optical materials, transparent in a wide range of the spectrum from UV to IR [18, 19], as well as matrices for doping with active rare earth ions [20-24]. There are no questions about the technological stability of the relevant materials. Continuous solid solutions of  $\text{Ca}_{1-x}\text{Sr}_x\text{F}_2$  is obtained even when using low-temperature synthesis methods, including co-precipitation from aqueous solutions [25].

Another example is the  $\text{CaF}_2$  -  $\text{BaF}_2$  system.

Preliminary studies have shown that the picture of phase equilibria in the system is more complex than described in [26]. The system contains intermediate phases stable within a narrow temperature range.

Limited solid solutions based on the components are formed in the system. Both the growth of single crystals from the melt [27] and

low-temperature co-precipitation [25] allow the synthesis of only limited solid solutions. However, the  $\text{Ba}_{1-x}\text{Ca}_x\text{F}_2$  continuous solid solution was obtained by mechanochemical synthesis [28]. The corresponding samples can exist for an indefinitely long period of time. However, after heating, the system transformed into an equilibrium state. The decomposition of the solid solution accompanied by the release of heat and an exothermic effect on thermograms at 420–450 °C occurs [29].

In general, the behavior of spinodals in complex cases remains unclear. Each specific case requires careful analysis.

The phase diagram of the  $\text{BaF}_2$ - $\text{LaF}_3$  system is shown in Fig. 4. At the phase diagram, using a special technique focused on the use of low-temperature phase formation, the immiscibility region of the  $\text{Ba}_{1-x}\text{La}_x\text{F}_{2+x}$  heterovalent solid solution was identified (phase *F*) [30]. The indicated position of the spinodal (Fig. 4b) shows that at room temperature the  $\text{Ba}_{1-x}\text{La}_x\text{F}_{2+x}$  solid solution is in a labile state in the approximate concentration range of  $0.03 < x < 0.45$ . This

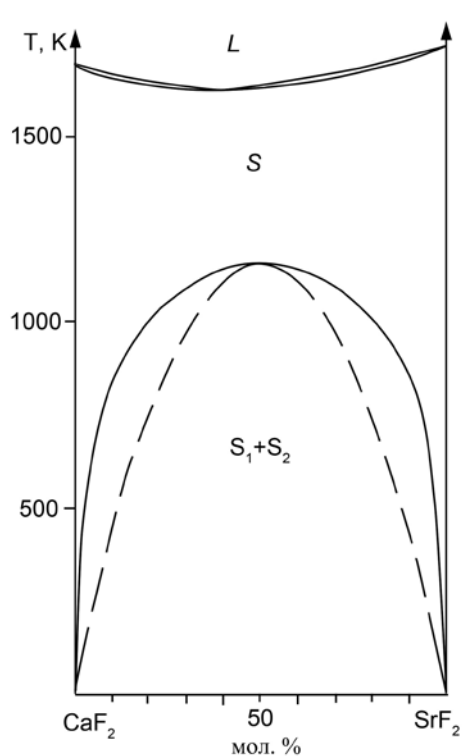


Fig. 3. Phase diagram of the  $\text{CaF}_2$ - $\text{SrF}_2$  system [16]

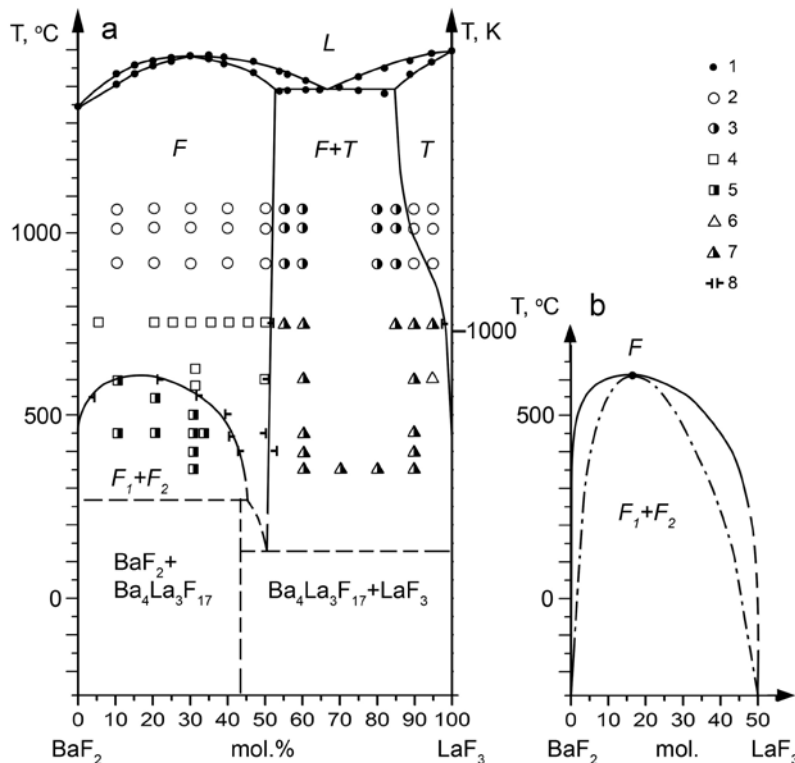


Fig. 4. Phase diagram of the  $\text{BaF}_2$ - $\text{LaF}_3$  system [30] (a), and the proposed region of spinodal decomposition of the solid solution (dash-dotted line, b). 1-3 – data from Sobolev and Tkachenko [30]



qualitatively corresponds to the results of the synthesis of solid solutions by co-precipitation of fluorides from aqueous solutions [32]. However, the practical stability of the  $\text{Ba}_{1-x}\text{La}_x\text{F}_{2+2x}$  single crystals, grown from the melt is obvious. In particular, a composition containing 30 mol. %  $\text{LaF}_3$  is a promising multifunctional material [33].

The next example is the  $\text{SrF}_2$ - $\text{LaF}_3$  system (Fig. 5) [34]. The low-temperature studies have shown that the homogeneity region of the  $\text{Sr}_{1-x}\text{La}_x\text{F}_{2+2x}$  fluorite solid solution below 400 °C rapidly decreases and almost reaches zero, which corresponds to the requirements of the third law of thermodynamics [35, 36] (Fig. 5). How can the spinodal be located for such a decomposition of the  $\text{Sr}_{1-x}\text{La}_x\text{F}_{2+2x}$  solid solution?

In this case, the solvus curve has an inflection point with a practically horizontal tangent. According to the van der Waals equation for coexisting phases in a binary system at constant pressure [35, 37]:

$$(\partial T/\partial x)_p = \Delta x (\partial^2 G/\partial x^2)_{p,T} / [\Delta x (\partial S/\partial x)_{p,T} - \Delta S]. \quad (5)$$

In this equation, the derivatives of the isobaric-isothermal potential  $G$  and entropy  $S$  for the concentration  $x$  of any component in the considered solid solution are used. The  $\Delta x$  and  $\Delta S$  values are equal to the difference in concentrations and entropies of coexisting phases. From this equation it follows that the horizontal tangent to the equilibrium curve of two phases  $(\partial T/\partial x)_p = 0$  can occur if  $\Delta x = 0$  or  $(\partial^2 G/\partial x^2)_{p,T} = 0$ . The first condition corresponds to the equality of the compositions of two phases that are in equilibrium and does not correspond to the considered case. The second variant remains.

Thus, the presence of a horizontal tangent to the solvus curve corresponds to the boundary condition of stability with respect to diffusion. In [34], the approach of a diffuse phase transition in the  $\text{Sr}_{1-x}\text{La}_x\text{F}_{2+2x}$  solid solution from above to the solvus curve was proposed. However, this was not confirmed by the recording of DSC curves. Thus, the approach from below the binodal curve of metastable immiscibility of the  $\text{Sr}_{1-x}\text{La}_x\text{F}_{2+2x}$  solid solution in a way that the critical point practically coincides with the solvus curve, presented in Fig. 6c, remains. Such a critical state of phase equilibria, changing the topology of the phase

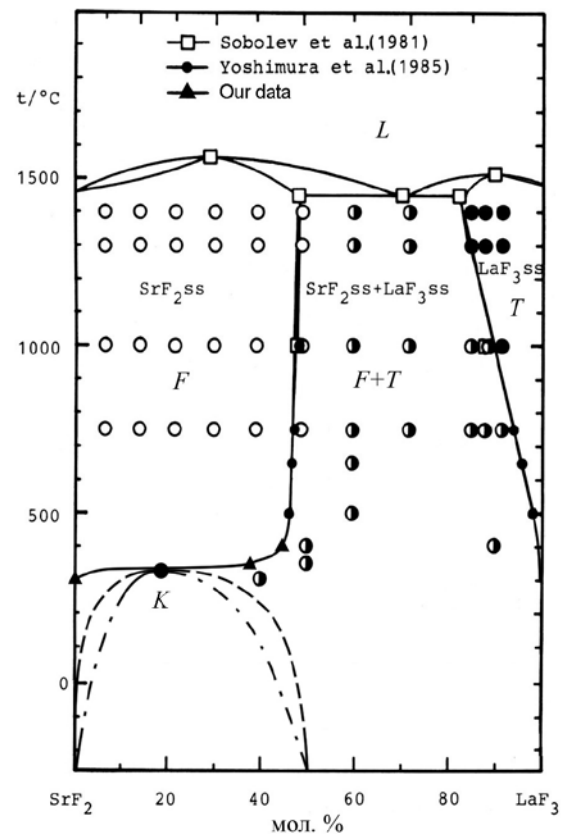


**Fig. 5.** Phase diagram of the  $\text{SrF}_2$ - $\text{LaF}_3$  system [34] and the probable position of the binodal (dotted line) and spinodal (dash-dotted line) in the region of metastable stability of the  $\text{Sr}_{1-x}\text{La}_x\text{F}_{2+2x}$  solid solution

diagram, is a bifurcation of the phase diagram [38, 39]. At the  $K$  critical point three lines with a horizontal tangent exist, namely: the solvus curve of the solid solution, the binodal of the metastable decomposition of this solid solution, and the spinodal corresponding to this binodal converge (Fig. 5).

Position of the  $\text{SrF}_2$ - $\text{LaF}_3$  system in the series shown in Fig. 6, practically corresponds to the bifurcation point (Fig. 6c), while the position of the  $\text{BaF}_2$ - $\text{LaF}_3$  system corresponds to Fig. 6d. Since the nature of phase equilibria in the vicinity of bifurcation points is subject to fluctuations [40], it is possible that variant (6d) is also implemented for the  $\text{SrF}_2$ - $\text{LaF}_3$  system with a slight excess of the critical immiscibility point of the solid solution over the solvus curve.

Approximate position of the spinodal in the  $\text{SrF}_2$ - $\text{LaF}_3$  system is shown in Fig. 5. Again, there are no problems with the stability of  $\text{Sr}_{1-x}\text{La}_x\text{F}_{2+2x}$  single crystals, grown from the melt. This also applies to a single crystal of the  $\text{Sr}_{0.70}\text{La}_{0.30}\text{F}_{2.30}$  composition, the

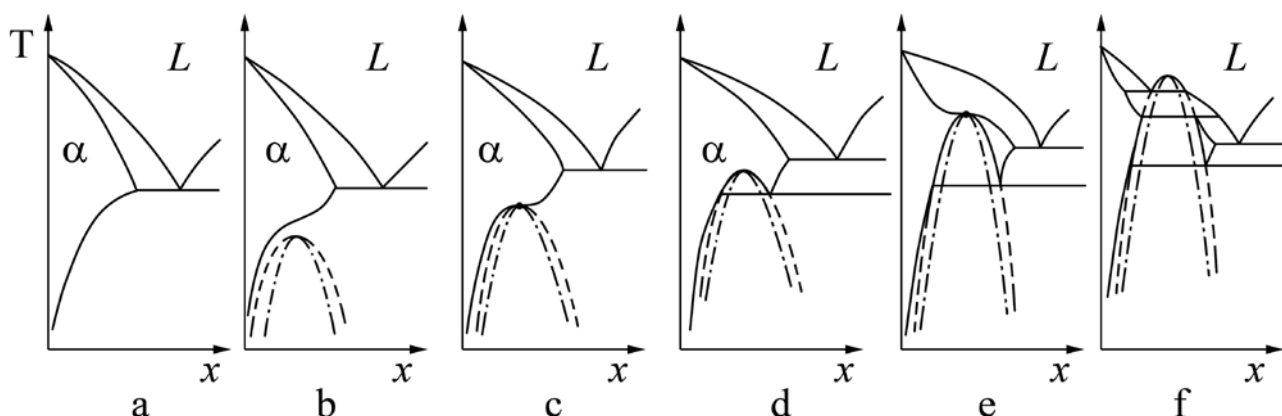


**Fig. 6.** Change in the phase diagram of a binary system due to an increase in the critical temperature of solid solution immiscibility (“sunrise-sunset” bifurcation) [38]. Dotted line – metastable equilibria, dash-dotted line – spinodals

most refractory inorganic fluoride with a melting temperature of 1570 °C [33].

The  $\text{BaF}_2\text{-RF}_3$  ( $R = \text{Pr, Nd}$ ) systems studied in the low-temperature region [41] are characterized by inflection points on the solvus curves. This indicates the presence of metastable low-temperature immiscibility of solid solutions. Probably, the corresponding phase diagrams occupy position (b) in the sequence diagram shown in Fig. 6, with metastable immiscibility of the fluorite solid solution (and the corresponding spinodal) at a lower temperature. The assumption of the presence of low-temperature spinodal decomposition of the  $\text{Ba}_{1-x}\text{R}_x\text{F}_{2+2x}$  solid solutions is confirmed by the results of attempts to synthesize the corresponding solid solutions by co-precipitation from aqueous solutions [32]: as a result of the synthesis, a mixture of practically pure barium fluoride and a fluorite phase containing about 40 mol. %  $\text{RF}_3$  was formed.

Finally, we will discuss systems of zirconium dioxide with oxides of rare earth elements, which are sources of optical materials – cubic zirconia (fianite) [42, 43]. Continuation of the curves of the limiting solubility of solid solutions based on the high-temperature  $\text{ZrO}_2$  modification into the region of low temperatures [44], taking into account the requirement of the presence of a vertical tangent at a temperature approaching absolute zero [45], inevitably requires the presence of an inflection point on the metastable solvus curve, see Fig. 8. Based on the above description, this also indicates metastable immiscibility of the  $\text{Zr}_{1-x}\text{R}_x\text{O}_{2-0.5x}$  solid solutions,

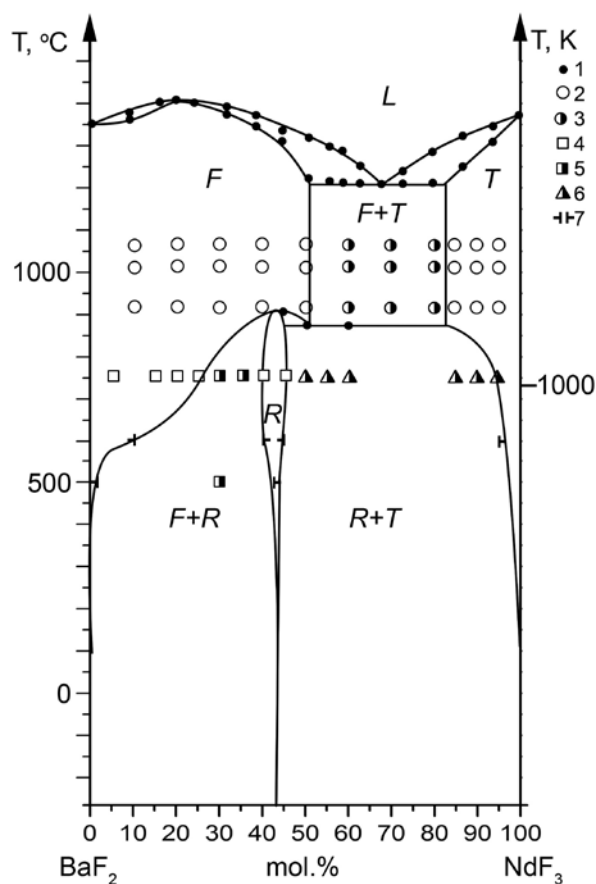


**Fig. 7.** Phase diagram of the  $\text{BaF}_2\text{-NdF}_3$  system [41]. 1–3 – data [31]

which, however, occurs at very low temperatures, possibly below room temperature.

#### 4. Architecture of spinodal decomposition

Single-phase materials located in the spinodal decomposition zone must undergo a directed evolution, consisting of decomposition into

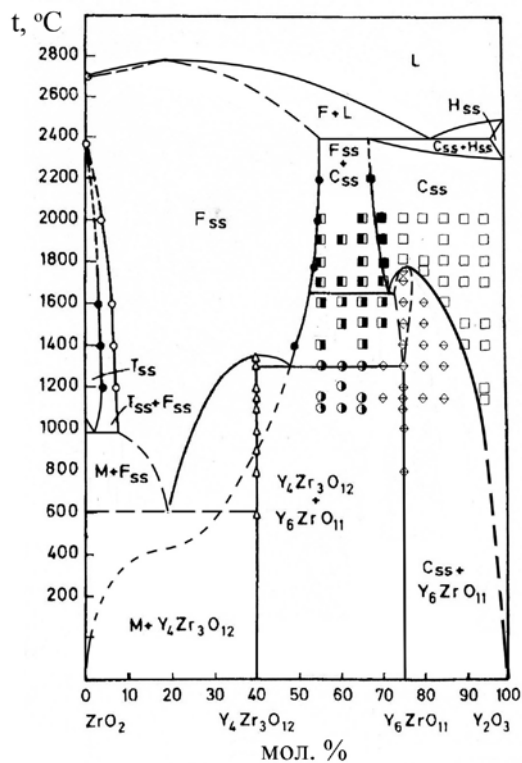


Fig. 8. Phase diagram of the  $ZrO_2$ - $Y_2O_3$  system [42]

two phases, and this process must occur with acceleration. The differences in the coexisting phases and the characteristic size of each of them continuously increase. The structure of the resulting aggregate has a complex topology and is the subject of numerous computational and experimental studies, see, for example, [12, 46-51]. In mathematical modelling, the Cahn-Hilliard equation is usually used. The corresponding materials have a set of topological, mechanical and physicochemical properties that determine the interest in such objects. Such terms as two-framework structures [12], spinoidal metamaterials [49, 50], spinodal architected materials [51], multifunctional spinodal nanoarchitectures [45], self-assembled nanolabyrinthine materials [48], cellular materials with spinodal topologies [47] are used for these materials. These materials are stressed nanocomposites. Surprisingly, the topology of spinodal decomposition resembles the architecture of chalcedons [52].

However, we are primarily interested in single-phase materials in the spinodal decomposition zone. It should be noted that the answer to

the question: is the material homogeneous? – mainly depends on the used research methods. In optically transparent single crystals of the  $Ba_{1-x}R_xF_{2+x}$  solid solutions, discussed above, heterogeneities of the order of  $\sim 20$  nm in size were revealed by electron microscopy [33, 53]. However, the quality of single crystals allows laser generation to be obtained even after long-term storage. An example of an optical quality single crystal after storage for about 40 years is shown in Fig. 9. It should be noted that the expected size of the inhomogeneity is approximately an order of magnitude smaller than the wavelength of light. In this case, according to the X-ray diffraction method, such samples are single-phase, with well-defined unit cell parameters, linearly dependent on the composition. At the same time, when these crystals were studied using the Raman light scattering method, they look more like two-phase systems. This issue requires further investigation.



Fig. 9. Single crystal of  $Ba_{0.71}Nd_{0.29}F_{2.29}$  – optical filter for a wavelength of  $2.5 \mu m$ . The faceting is artificial. Grown by T. Turkina [54]. Photographed January 22, 2024

Electron microscopy did not reveal inhomogeneities similar to those described for single crystals of the  $Ba_{1-x}R_xF_{2+x}$  solid solutions in single crystals of cubic zirconia with a concentration of about 10 mol. %  $Y_2O_3$ .

## 5. Conclusions

Thus, the conducted analysis of phase diagrams shows that solid solutions with a fluorite structure, such as  $M_{1-x}R_xF_{2+x}$  ( $M = Ca, Sr,$  or  $Ba$ ) fluorides and  $Zr_{1-x}R_xO_{2-0.5x}$  ( $R =$  rare earth), are labile at normal temperature and pressure, but they do not show degradation corresponding to spinodal decomposition. The same applies to functional materials created on their basis:



their technological stability is much higher than thermodynamic stability [55]. Obviously, this is determined by the extremely low values of the diffusion coefficients of cations. The systems are “falling”, but too slowly to be noticed.

Fig. 9, which records the preservation of functional material in a labile state for approximately 40 years, convincingly refutes Gukhman’s assertion [4]. Obsidian (volcanic glass), existing in a thermodynamically non-equilibrium state, was a functional material of Paleolithic cultures for thousands of years. Some manifestations of volcanic glass retain its original amorphous (apparently labile) form for 200 million years [56].

### Conflict of interests

The author declares that he has no known financial conflicts of interest or personal relationships that could have influenced the work presented in this article.

### References

- Gibbs J. V. *Thermodynamic works\**. Moscow; Leningrad: GITTL Publ., 1950. 492 p. (In Russ.)
- Storonkin A. V. *Thermodynamics of heterogeneous systems\**. Leningrad: Leningrad State University Publ., 1967. 447 p. (In Russ.)
- Prigogin I., Defay R. D. *Chemical thermodynamics*. Longman Green and Co. London et al., 1954. 533 p.
- Gukhman A. A. *On the foundations of thermodynamics\**. Moscow: URSS Publ., 2010. 384 p. (In Russ.)
- Rusanov A. I. *Phase equilibria and surface phenomena\**. Leningrad: Khimiya Publ., 1967. 388 p. (In Russ.)
- Münster A. *Chemische thermodynamik*. Berlin: Akademie Verlag; 1969.
- Landau L. D., Lifshitz E. M. *Statistical physics\**. Vol. 1. Moscow: Nauka Publ., 586 p. (In Russ.)
- Cahn J. W. *Spinodal decomposition. The 1967 Institute of Metals Lecture*. TMS AIME 1968;242; 166–180. <https://doi.org/10.1002/9781118788295.ch10>
- Cahn J. W., Charles R. J. The initial stages of phase separation in glasses. *Physics and Chemistry of Glasses*. 1965;6(5): 181–191.
- Carpenter M. A. A “conditional spinodal” within the peristerite miscibility gap of plagioclase feldspars. *American Mineralogist*. 1981;66: 553–560. Available at: [http://www.minsocam.org/ammin/AM66/AM66\\_553.pdf](http://www.minsocam.org/ammin/AM66/AM66_553.pdf)
- Uhlmann D. R., Kolbeck A. G. Phase separation and the revolution in concepts of glass structure. *Physics and Chemistry of Glasses*. 1976;17(5): 146–158.
- Mazurin O. V., Roskova G. P., Averyanov V. I., Antropova T. V. *Two-phase glasses: structure, properties, application\**. Leningrad: Nauka Publ.; 1991. 276 p. (In Russ.)
- Bhardwaj M. C., Roy R. Effect of high pressure on crystalline solubility in the system NaCl-KCl. *Journal of Physics and Chemistry of Solids*. 1971;32: 1693–1607. [https://doi.org/10.1016/s0022-3697\(71\)80053-7](https://doi.org/10.1016/s0022-3697(71)80053-7)
- Schiraldi A., Pezzati E., Chiodelli G. Phase diagram and point defect parameters of the system CsBr-TlBr. *Zeitschrift für Physikalische Chemie*. 1978;110: 1–16. <https://doi.org/10.1524/zpch.1978.110.1.001>
- Eliseev A. A., Lukashin A. V., Vertigel A. A. Cryosol synthesis of  $Al_{2-x}Cr_xO_3$  solid solutions. *Chemistry of Materials*. 1999;11: 241–246. <https://doi.org/10.1021/cm9807211>
- Fedorov P. P., Mayakova M. N., Alexandrov A. A., ... Ivanov V. K. The melt of sodium nitrate as a medium for synthesis of fluorides. *Inorganics*. 2018;6(2): 38–55. <https://doi.org/10.3390/inorganics6020038>
- Ol'khovaya L. A., Karpenko G. A., Ikrami D. D., Fedorov P. P. The  $CaF_2$ - $SrF_2$ - $MnF_2$  ternary system. *Russian Journal of Inorganic Chemistry*. 1991;36(11): 1639–1642.
- Popov P. A., Moiseev N. V., Karimov D. N., ... Fedorov P. P. Thermophysical characteristics of  $Ca_{1-x}Sr_xF_2$  solid-solution crystals ( $0 \leq x \leq 1$ ). *Crystallography Reports*. 2015;60(1): 116–122.
- Takahashi K., Cadatal-Raduban M., Sarukura N., Kawamata T., Sugiyama K., Fukuda T. Crystal growth and characterization of large  $Ca_{0.582}Sr_{0.418}F_2$  single crystal by Czochralski method using cone die. *Journal of Crystal Growth*. 2024;628: 127541. <https://doi.org/10.1016/j.jcrysgro.2023.127541>
- Basiev T. T., Vasil'ev S. V., Doroshenko M. E., ... Fedorov P. P. Efficient lasing in diode-pumped  $Yb^{3+}:CaF_2$ - $SrF_2$  solid-solution single crystals. *Quantum Electronics*. 2007;37(10): 934–937. <https://doi.org/10.1070/qe2007v037n10abeh013662>
- Ushakov S. N., Uslamina M. A., Nishchev K. N., ... Osiko V. V. Study of  $Yb^{3+}$  optical centers in fluoride solid solution crystals  $CaF_2$ - $SrF_2$ - $YbF_3$ . *Optics and Spectroscopy*. 2020;128(5): 600–604. <https://doi.org/10.1134/S0030400X20050185>
- Kuznetsov S. V., Konyushkin V. A., Nakladov A. N., ... Fedorov P. P. Thermophysical properties of single crystals of  $CaF_2$ - $SrF_2$ - $RF_3$  ( $R = Ho, Pr$ ) fluorite solid solutions. *Inorganic Materials*. 2020;56(9): 975–981. <https://doi.org/10.1134/s0020168520090113>
- Normani S., Loiko P., Basyrova L., ... Camy P. Mid-infrared emission properties of erbium-doped fluorite-type crystals. *Optical Materials Express*. 2023;13(7): 1836–1850. <https://doi.org/10.1364/ome.482402>
- Zhu C., Song J., Mei B., Li W., Liu Z. Fabrication and optical characterizations of  $CaF_2$ - $SrF_2$ - $NdF_3$  transparent ceramics. *Materials Letters* 2016;167(10): 115–117. <https://doi.org/10.1016/j.matlet.2015.12.083>
- Fedorov P. P., Kuznetsov S. V., Mayakova M. N., ... Osiko V. V. Coprecipitation from aqueous solutions to prepare binary fluorides. *Russian Journal of Inorganic Chemistry*. 2011;56(10): 1525–1531. <https://doi.org/10.1134/S003602361110007X>
- Fedorov P. P., Buchinskaya I. I., Ivanovskaya N. A., Konovalova V. V., Lavrishchev S. V., Sobolev B. P.  $CaF_2$ - $BaF_2$  phase diagram. *Doklady Physical Chemistry*. 2005;401(2): 53–55. <https://doi.org/10.1007/s10634-005-0024-5>
- Wrubel G. P., Hubbard B. E., Agladze N. I., ... Campbell G. A. Glasslike two-level systems in minimally disordered mixed crystals. *Physical Review Letters*. 2006;96: 235503. <https://doi.org/10.1103/PhysRevLett.96.235503>



28. Heise M., Scholz G., Düvel A., Heitjans P., Kemnitz E. Mechanochemical synthesis, structure, and properties of solid solutions of alkaline earth metal fluorides:  $M_{1-x}^a M_x^b F_2$  ( $M$ : Ca, Sr, Ba). *Solid State Sciences*. 2016;60: 65–74. <https://doi.org/10.1016/j.solidstatesciences.2016.08.004>
29. Düvel A., Heitjans P., Fedorov P. P., Voronov V. V., Pynenkov A. A., Nishchev K. N. Thermal stability of  $Ca_{1-x}Ba_xF_2$  solid solution. *Solid State Science*. 2018;83: 188–191. <https://doi.org/10.1016/j.solidstatesciences.2018.05.011>
30. Aleksandrov A. A., Shevchenko A. G., Sorokin N. I., ... Fedorov P. P. Phase equilibria in the BaF–LaF<sub>3</sub> system\*. In: *Abstracts of the scientific and practical conference “Fluoride materials and technologies”, April 15–19, Moscow, 2024*. Moscow: FSRC “Crystallography and photonics” of NRC «Kurchatov Institute» RAS; 2024. pp. 111–112. Available at: <https://fluorchem.ru/>
31. Sobolev B. P., Tkachenko N. L. Phase diagrams of BaF<sub>2</sub>–(Y, Ln)F<sub>3</sub> systems. *Journal of Less-Common Metals*. 1982;85: 155. [https://doi.org/10.1016/0022-5088\(82\)90067-4](https://doi.org/10.1016/0022-5088(82)90067-4)
32. Kuznetsov S. V., Fedorov P. P., Voronov V. V., Samarina K. S., Ermakov R. P., Osiko V. V. Synthesis of Ba<sub>1-x</sub>R<sub>3x</sub>F<sub>17</sub> (R stands for rare-earth elements) powders and transparent compacts on their base. *Russian Journal of Inorganic Chemistry*. 2010;55(4): 484–493. <https://doi.org/10.1134/S0036023610040029>
33. Sobolev B. P. *The rare earth trifluorides. Part 2*. Introduction to materials science of multicomponent metal fluoride crystals. Barcelona: Institut d’Estudis Catalans; 2001.
34. Fedorov P. P., Alexandrov A. A., Voronov V. V., Mayakova M. N., Baranchikov A. E., Ivanov V. K. Low-temperature phase formation in the SrF<sub>2</sub>–LaF<sub>3</sub> system. *Journal of the American Ceramic Society*. 2021;104(6): 2836–2848. <https://doi.org/10.1111/jace.17666>
35. Fedorov P. P. Third law of thermodynamics as applied to phase diagrams. *Russian Journal of Inorganic Chemistry*. 2010;55(11): 1722–1739. <https://doi.org/10.1134/S0036023610110100>
36. Laughlin D. E., Soffa W. A. The third law of thermodynamics: phase equilibria and phase diagrams at low temperatures. *Acta Materialia*. 2018;45: 49–61. <https://doi.org/10.1016/j.actamat.2017.11.037>
37. van der Waals J. D., Konstamm PH. *Lehrbuch der thermostatik*. Leipzig: verlag von Johann Ambrosius Bath; 1927.
38. Fedorov P. P. Factors responsible for the appearance of inflections in solid-solution demixing curves. *Russian Journal of Inorganic Chemistry*. 2001;46(10): 1567–1570.
39. Fedorov P. P. Transformations of  $T$ - $x$  phase diagrams of binary systems in the condensed state: II. Phase equilibria under constraints. *Russian journal of Physical Chemistry A*. 1999;73(9): 1387–1392. Available at: <https://elibrary.ru/item.asp?id=13311944>
40. Fedorov P. P., Medvedeva L. V., Sobolev B. P. Bifurcations in the  $T$ - $x$  phase diagrams of binary systems in the condensed state. Fluctuations of the phase transition type in the LiF–YF<sub>3</sub> system. *Russian journal of Physical Chemistry A*. 2002;76(3): 337–342. Available at: <https://elibrary.ru/item.asp?id=13407836>
41. Fedorov P. P., Alexandrov A. A., Luginina A. A., Voronov V. V., Kuznetsov S. V., Chernova E. V. Phase diagrams of the BaF<sub>2</sub> – NdF<sub>3</sub> and BaF<sub>2</sub> – PrF<sub>3</sub> systems. *Journal of the American Ceramic Society*. 2024. <https://doi.org/10.1111/jace.20152>
42. Fedorov P. P.,\* Yarotskaya E. G. Zirconium dioxide. Review. *Condensed Matter and Interphases*. 2021;23(2): 169–187. <https://doi.org/10.17308/kcmf.2021.23/3427>
43. Fedorov P. P. Phase equilibria in low-temperature regions of phase diagrams. *Journal of Phase Equilibria and Diffusion*. 2024;45(3): 475–488. <https://doi.org/10.1007/s11669-024-01099-7>
44. P. P. Fedorov, E. V. Chernova. Phase diagrams of zirconia systems with yttria and scandia. *Condensed Matter and Interphases*. 2023;25(2): 257–267. <https://doi.org/10.17308/kcmf.2023.25/11106>
45. Laughlin D. E., Massalski T. B. Construction of equilibrium phase diagrams: Some errors to be avoided. *Progress in Materials Science*. 2020;120: 100715. <http://doi.org/10.1016/j.pmatsci.2020.100715>
46. Guell Izard A., Bauer J., Crook C., Turlo V., Valdevit L. Ultrahigh energy absorption multifunctional spinodal nanoarchitectures. *Small*. 2019;15(45): 1903834. <https://doi.org/10.1002/sml.201903834>
47. Hsieh M.-T., Endo B., Zhang Y., Bauer J., Valdevit L. The mechanical response of cellular materials with spinodal topologies. *Journal of the Mechanics and Physics of Solids*. 2019;125: 401–419. <http://doi.org/10.1016/j.jmps.2019.01.002>
48. Portela C. M., Vidyasagar A., Krödel S., ... Kochmann D. M. Extreme mechanical resilience of self-assembled nanolabyrinthine materials. *Proceedings of the National Academy of Sciences*. 2020;117(11): 5686–5693. <http://doi.org/10.1073/pnas.1916817117>
49. Zheng L., Kumar S., Kochmann D. M. Data-driven topology optimization of spinodoid metamaterials with seamlessly tunable anisotropy. *Computer Methods in Applied Mechanics and Engineering*. 2021;383: 113894. <http://doi.org/10.1016/j.cma.2021.113894>
50. Kumar S., Tan S., Zheng L., Kochmann D. M. Inverse-designed spinodoid metamaterials. *npj Computational Materials*. 2020;6(1): 73. <http://doi.org/10.1038/s41524-020-0341-6>
51. Senhora F. V., Sanders E. D., Paulino G. H. Optimally-tailored spinodal architected materials for multiscale design and manufacturing. *Advanced Materials*. 2022;34(26): 2109304. <https://doi.org/10.1002/adma.202109304>
52. Gaynutdinov R., Voronov V. V., Chernova E. V., ... Fedorov P. P. Flints as nanostructured chalcedons. *Journal of Surface Investigation: X-ray, Synchrotron and Neutron Techniques*. 2020;14(4): 762–770. <https://doi.org/10.1134/S1027451020040084>
53. Nikolaiichik V. I., Sobolev B. P., Sorokin N. I., Avilov A. S. Electron diffraction study and ionic conductivity of fluorite Ba<sub>1-x</sub>La<sub>x</sub>F<sub>2+2x</sub> and tysonite La<sub>1-y</sub>Ba<sub>y</sub>F<sub>3-y</sub> phases in the BaF<sub>2</sub>–LaF<sub>3</sub> system. *Solid State Ionics*. 2022;386: 116052. <https://doi.org/10.1016/j.ssi.2022.116052>
54. Turkina T. *Morphological stability of the crystallization front of solid  $M_{1-x}R_xF_{2+2x}$  solutions (where  $M = Ca, Sr, Ba, R - REM$ )*\*. Cand. Sci. (Phys.-Math.) thesis. Moscow: Institute of

Crystallography, USSR Academy of Sciences. 1990. Available at: <https://search.rsl.ru/ru/record/01000054976>

55. Fedorov P. P. Nanotechnology and material science. *Nanosystems: Physics, Chemistry, Mathematics*. 2020;11(3): 314–315, <https://doi.org/10.17586/2220-8054-2020-11-3-314-315>

56. Lebedinsky V. I. *Volcanic crown of the great plain\**. Moscow: Nauka Publ.; 1973. 192 p.

\* Translated by author of the article

### Information about the author

*Pavel P. Fedorov*, Dr. Sci. (Chem.), Full Professor, Chief Researcher at the Prokhorov General Physics Institute of the Russian Academy of Sciences (Moscow, Russian Federation).

<https://orcid.org/0000-0002-2918-3926>

[ppfedorov@yandex.ru](mailto:ppfedorov@yandex.ru)

Received 24.07.2024; approved after reviewing 24.09.2024; accepted for publication 16.09.2024; published online 25.12.2024.

Translated by Valentina Mittova